

## Further Insights into the Electrooxidation of *N*-Methyluric Acids and Correlation of Oxidation Potentials with Frontier MO Energies

Rajendra N. Goyal,\* P. P. Thankachan, and Neena Jain

Department of Chemistry, University of Roorkee, Roorkee 247667, India

(Received November 8, 1999)

The electrochemical oxidation of various *N*-methylated uric acids has been studied at a pyrolytic graphite electrode at physiological pH 7.2. The observed behavior was compared with uric acid to evaluate the effect of a methyl group. The  $E_p$  value was found to shift to less positive potentials when a methyl group is present at the N-1 position and to more positive potentials when substitution is at the N-3 position or at nitrogens of the imidazole ring. The values of  $\Delta E_p$  followed the additivity of the substituents effect only when two methyl groups are present in different rings. The methyl groups were also found to increase the electron density at N atoms of uric acids, and an excellent correlation between the oxidation potential and energy of the highest occupied molecular orbital was observed. On the basis of these studies it is concluded that the presence of a methyl group in the pyrimidine ring restricts the formation of allantoin. The peroxidase-catalysed oxidation of the *N*-methylated derivatives of uric acid was found to follow a pathway similar to that observed during electrochemical oxidation.

Uric acid, one of the major end products of purine catabolism in humans,<sup>1</sup> has also been found to be a constituent of many body fluids, particularly human urine and urinary calculi. The extreme abnormalities of the uric acid level in body fluids are indicative of certain diseases.<sup>2,3</sup> The difference in the concentration of uric acid in blood serum before and after exercise has been used as a measure of nucleotide degradation.<sup>4</sup> Uric acid also provides an antioxidant defense in humans against oxidant and radical-caused aging and cancer.<sup>5</sup> Some of the products of uric acid oxidation in the human system have been found to be toxic in nature,<sup>6</sup> which has lead to extensive investigations on purines and related compounds.

The presence of an alkyl group in purines not only affects the ease of oxidation by changing the electron density at various atoms, but also alters the mechanism.<sup>7</sup> The methylation of purines significantly influences the stacking intermediate between the parent molecules of nucleic acid bases, and thus their plane-to-plane association structures.<sup>8</sup> Alkylated purines are also known to be antagonists of adenosine receptors.<sup>9,10</sup> Many of the methylated purines are pharmacologically important and are useful in the treatment of asthma and urinary-tract diseases.<sup>11</sup> Methyl xanthines have been claimed to possess the ability to override the mitotic block in human tumour cells.<sup>12</sup> It has been reported that Apnea, or sudden infant death syndrome (SIDS), can be effectively treated by methylated purine derivatives.<sup>13</sup> The methylated analogs of uric acid have also shown high potency in the prevention of lipid peroxidation, and may thus be useful as antioxidants.<sup>14</sup> Attempts have been made to determine uric acids in various biological fluids by voltammetric and related techniques.<sup>15–19</sup> However, very few efforts have been made to elucidate the mechanistic redox chemistry<sup>20</sup> of such

molecules with special reference to the effect of methylation on ease of oxidation. In view of this, a study of the redox behavior of various *N*-methylated analogs of uric acid was initiated in our laboratory.<sup>21</sup> The main thrust in these studies was to determine the extent to which the basic mechanism of uric acid oxidation is altered upon methylation. Molecular-orbital calculations have been recognized to be a powerful method to study the intermolecular interaction potentials of organic molecules. It was thus considered desirable to calculate the electron density at various atoms and the energy of the highest occupied molecular orbital. This present paper deals with a comparative study on the electrochemical and enzymic oxidation of various mono-, di-, and tri-substituted uric acids at pH 7.2. The effect of introducing a methyl group at different positions in the pyrimidine and imidazole ring as well as the overall impact of increasing the number of methyl groups in uric acid on the electrochemical and enzymic behavior of the parent compound (**I**) is discussed. Because molecular orbital studies have been found to be useful in correlating the structure of a variety of organic compounds,<sup>22</sup> the peak potentials of various uric acids have also been correlated with the energy of the highest occupied molecular orbital obtained using the MNDO programme. It is believed that these studies will help us to fully understand the influence of methyl groups on the oxidation mechanism of these biomolecules at the electrode solution interface.

### Experimental

Uric acid was procured from Calbiochem, USA and *N*-methylated uric acids were obtained from Adams Chemical Company, USA. All of the compounds were used as received. Type-VIII peroxidase ( $R_z \approx 3.4$ ) and catalase were the products of Sigma Chemical Company, USA. A stock solution of uric acids (1 mM)

was prepared in double-distilled water ( $1\text{ M} = 1\text{ mol dm}^{-3}$ ). All of the experiments were carried out in phosphate buffers<sup>23</sup> of pH 7.2 ( $\mu = 0.5\text{ M}$ ). The equipment used and procedures for voltammetry, controlled potential electrolysis, coulometry, and spectral studies have been described elsewhere.<sup>21</sup> All of the potentials were referred to the SCE at an ambient temperature of  $25 \pm 1^\circ\text{C}$ . The method used for fabricating a pyrolytic graphite electrode (area of ca.  $9\text{ mm}^2$ ) was essentially the same as that described earlier.<sup>21</sup> The electrode surface was cleaned each time by rubbing on emery paper before recording the voltammogram. This procedure resulted in a different surface area each time, and hence the  $i_p$  values were calculated as an average of at least three curves. The values of  $n$ , the number of electrons involved in oxidation, were determined by graphical integration of the current–time curve, as reported by Lingane.<sup>24</sup>

The enzymic oxidation of uric acids was carried out by using fresh solutions of peroxidase ( $0.002\text{ mM}$ ) and  $\text{H}_2\text{O}_2$  ( $0.6\text{ mM}$ ). All solutions were prepared in phosphate buffers of  $7.2\text{ pH}$ . A  $2\text{ ml}$  solution of appropriate uric acid was mixed with  $0.5\text{ ml}$  of horseradish peroxidase. The oxidation was initiated by adding  $0.5\text{ ml}$  of  $\text{H}_2\text{O}_2$ . The course of the reaction was monitored by repeatedly scanning the UV/vis-spectra of the resulting solution. In another set, when the absorbance at  $\lambda_{\text{max}}$  reached 50%, the reaction was terminated by the addition of  $0.1\text{ ml}$  of a catalase solution ( $1\text{ mg ml}^{-1}$ ). This amount of catalase was sufficient to rapidly remove  $\text{H}_2\text{O}_2$  from the reaction mixture. The spectra were again monitored at different time intervals. For studying the kinetics of the decay of the intermediate, the change in the absorbance at selected wavelengths was monitored as a function of time.

The products of electrooxidation were obtained by exhaustively electrolyzing about  $10\text{ mg}$  of a compound in an H-cell at the peak  $I_a$  potentials. The products obtained after lyophilization were separated by gel permeation chromatography using a glass column packed with Sephadex G-10 (Sigma, bead size  $40\text{--}120\text{ }\mu\text{mol dm}^{-3}$ ). Double-distilled water was used as an eluent and fractions of  $5\text{ ml}$  each were collected. The absorbance of the fractions was determined at  $210\text{ nm}$ . The first peak in gel-permeation chromatography was always found to contain phosphate, and was hence discarded. The other observed peaks were collected separately, lyophilized and analysed by mp, TLC, IR, and GC-mass.

MO calculations were performed using the MNDO programme developed by Dewar and co-workers<sup>25</sup> for use on an IBM PC. The initial geometry based on the X-ray results of Sutor<sup>26</sup> were input and optimised during the MNDO calculations. It was found that while the X-ray result suggests an almost planar geometry, the MNDO-optimised geometries were not strictly planar. Frontier orbital energies and atomic charges were obtained at the optimum geometry from these calculations.

## Results and Discussion

In the cyclic voltammetry of methylated uric acids at PGE at a sweep rate of  $100\text{ mV s}^{-1}$ , a well-defined peak ( $I_a$ ) was observed similar to that for unsubstituted uric acid (Fig. 1A). The  $E_p$  of peak  $I_a$  was dependent on the pH, and shifted to a less-positive potential with an increase in the pH. The values of  $dE_p/d\text{pH}$  observed for these compounds are presented in Table 1. In a reverse sweep, two reduction peaks,  $I_c$  and  $II_c$ , were observed in the case of compounds **II** to **VII** (Fig. 1B) and **IX** to **XII** (Figs. 1C and 1D). In the case of compound **VIII**, peak  $I_c$  was never noticed at  $7.2\text{ pH}$ . Peak  $I_c$  formed a quasi-reversible couple with peak  $I_a$ , as established by the

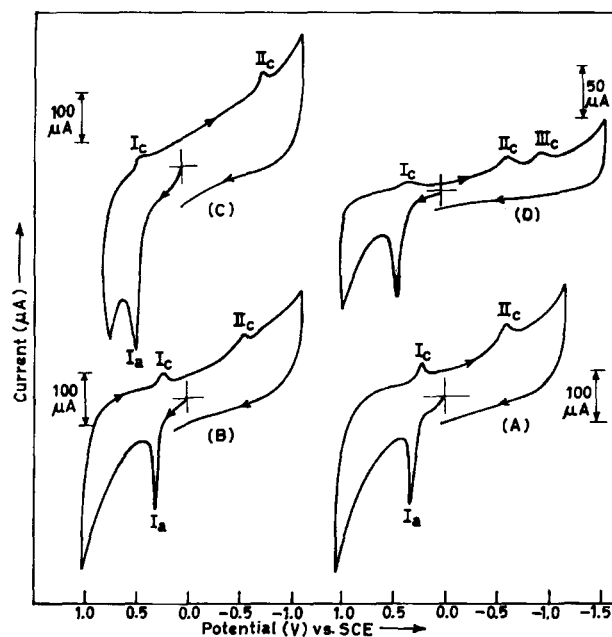


Fig. 1. A comparison of cyclic voltammograms of (A) uric acid (B) 3-methyluric acid (C) 7,9-dimethyluric acid (D) 1,3,7-trimethyluric acid at a sweep rate of  $100\text{ mV s}^{-1}$ ;  $\text{pH} = 7.2$ .

peak potential separation of the anodic and cathodic peaks at PGE. The peak potential separation of  $(E_p)_a$  and  $(E_p)_c$  varied over the range  $25\text{--}50\text{ mV}$  for all compounds at a sweep rate of  $100\text{ mV s}^{-1}$ , and is given in Table 1. The peak separation increased along with an increase in the sweep rate, and reached  $50\text{--}100\text{ mV}$  at  $1\text{ V s}^{-1}$ . The peak potential of reduction peaks  $I_c$  and  $II_c$  were also dependent on the pH, and shifted towards a more negative potential along with an increase in the pH in all compounds. 1,3-Dimethyluric acid (**VI**), 1,3,7-trimethyluric acid (**XI**) and 1,3,9-trimethyluric acid (**XII**) gave an additional reduction peak  $III_c$  at more negative potentials (Fig. 1D). It was interesting to observe that the peak current of peak  $I_c$  increased with an increase in the sweep rate in the range  $10\text{ mV s}^{-1}$  to  $1.0\text{ V s}^{-1}$  at PGE. The ratio of peaks  $I_c/I_a$  also increased with an increase in the sweep rate (Table 1). This behavior clearly indicates that the species responsible for peak  $I_c$  is unstable, and hence is more available in the vicinity of the electrode at higher sweep rates. Thus, it was confirmed that the electrode reaction is coupled with consecutive chemical reactions.<sup>27</sup>

The peak potential of peak  $I_a$  was also found to be dependent on the sweep rate, and shifted to a more positive potential by  $25\text{ mV}$  per ten-fold increase of the sweep rate in the sweep range  $5\text{ mV s}^{-1}$  to  $100\text{ mV s}^{-1}$  and by  $50\text{ mV}$  at a higher sweep range. The plots of the ratio of  $I_a/I_c$  vs.  $\log v$  and  $[(\Delta E_{p/2})/\Delta \log v]$  vs.  $\log v$  were S-shaped in all compounds, thereby establishing the EC nature of the electrode reaction in which charge transfer is followed by an irreversible chemical reaction.<sup>27</sup> The peak current for peak  $II_c$  was also found to be dependent on the sweep rate, and decreased along with an increase in the sweep rate as the oxidized species responsible for peak  $II_c$ , undergoes a chemical

Table 1. Comparison of Voltammetric Characteristics for Peaks  $I_a$  and  $I_c$  of 0.5 mM Uric Acids<sup>a)</sup> in Phosphate Buffer of pH 7.2

| No.  | Compound        |                 |                 |                 | $pK_a$ | $E_p$<br>mV | $(\Delta E_p)_a$<br>mV | $(E_p)_a - (E_p)_c$<br>mV | $I_c/I_a$              |                     |
|------|-----------------|-----------------|-----------------|-----------------|--------|-------------|------------------------|---------------------------|------------------------|---------------------|
|      | $R_1$           | $R_2$           | $R_3$           | $R_4$           |        |             |                        |                           | 100 mV s <sup>-1</sup> | 1 V s <sup>-1</sup> |
| I    | H               | H               | H               | H               | 5.7    | 300         | —                      | 25                        | 0.18                   | 0.64                |
| II   | CH <sub>3</sub> | H               | H               | H               | 6.0    | 290         | -10                    | 32                        | 0.22                   | 0.60                |
| III  | H               | CH <sub>3</sub> | H               | H               | 5.6    | 330         | +30                    | 35                        | 0.14                   | 0.33                |
| IV   | H               | H               | CH <sub>3</sub> | H               | 5.4    | 400         | +100                   | 37                        | 0.08                   | 0.27                |
| V    | H               | H               | H               | CH <sub>3</sub> | 4.5    | 350         | +50                    | 25                        | 0.20                   | 0.43                |
| VI   | CH <sub>3</sub> | CH <sub>3</sub> | H               | H               | 5.6    | 358         | +58                    | 30                        | 0.12                   | 0.24                |
| VII  | CH <sub>3</sub> | H               | CH <sub>3</sub> | H               | 5.5    | 410         | +110                   | 50                        | 0.20                   | 0.38                |
| VIII | H               | CH <sub>3</sub> | CH <sub>3</sub> | H               | 5.5    | 440         | +140                   | —                         | —                      | —                   |
| IX   | H               | CH <sub>3</sub> | H               | CH <sub>3</sub> | 5.2    | 370         | +70                    | 30                        | 0.05                   | 0.15                |
| X    | H               | H               | CH <sub>3</sub> | CH <sub>3</sub> | 5.6    | 490         | +190                   | 28                        | 0.05                   | 0.12                |
| XI   | CH <sub>3</sub> | CH <sub>3</sub> | CH <sub>3</sub> | H               | 6.0    | 460         | +160                   | 30                        | 0.20                   | 0.62                |
| XII  | CH <sub>3</sub> | CH <sub>3</sub> | H               | CH <sub>3</sub> | —      | 440         | +140                   | 42                        | 0.21                   | 0.60                |

a) Average of at least three replicate determinations.

follow up reaction, and hence is not available for a peak  $I_c$  reaction. The ratio of peaks  $I_c/I_a$  increased from ca. 0.9 at 100 mV s<sup>-1</sup> to ca. 1.2 at 1 V s<sup>-1</sup> at PGE in all of the compounds studied. The ratio of the peak currents for peaks  $I_c$  and  $I_a$  remained constant with an increase in the concentration of the compounds studied. This suggests that the species responsible for peak  $I_c$  is independent of the concentration of the reactant as well as to the primary oxidation product of the electrode reaction.

The peak-current values of peak  $I_a$  were also dependent on the concentration of *N*-methyluric acids. Thus,  $i_p$  increased with an increase in the concentration, and  $i_p$  vs. concentration plots were linear up to about 0.5 mM concentration; at higher concentrations the  $i_p$  values had a tendency to limit. This limiting nature of  $i_p$  clearly indicated a strong adsorption of the reactant at the surface of the electrode.<sup>27</sup> The spiky nature of the observed peaks also indicates adsorption of the reactants at the electrode surface.

An examination of the peak potential of  $I_a$  at pH 7.2 in Table 1 reflects that when a methyl group is present at the N-1 position the  $E_p$  value shifts to a less-positive potential in comparison to compound I. However, the methylation of uric acid at the N-3 position or in the imidazole ring (N-7 or N-9) causes a shift of the peak potential of peak  $I_a$  to more positive values. It was noticed that a shift in  $E_p$  to a more positive potential was larger whenever methyl substitution occurred in the imidazole ring. One of the possible reasons for such a large shift is the lack of dissociable hydrogen in these cases. The  $E_p$  of peak  $I_a$  for 7,9-dimethyluric acid (X) was 490 mV vs. SCE, and was highest among all of the uric acid derivatives studied. To quantitatively evaluate the effect of methyl groups on the ease of oxidation of uric acids, the values of  $\Delta E_p$  were calculated. The additive effect of methyl substituents was clearly noticed when the two methyl groups were in different rings. Thus, the 1,7-; 3,7-, and 3,9-

derivatives followed the additivity of the substituents effects, whereas when two methyl groups were present in the same ring a large deviation from the additivity was noticed, most probably due to a steric effect.<sup>28</sup>

The  $pK_a$  values, obtained spectrophotometrically for the methylated uric acids, were similar to the values reported in the literature,<sup>29,30</sup> and were comparable to that of uric acid. A comparison of  $pK_a$  and other voltammetric characteristics of various *N*-methyluric acids is presented in Table 1. In uric acid (I) and its *N*-methyl substituted derivatives, an anion is formed by the loss of a proton first from N-9 of the imidazole ring (Chart 1). If a methyl group is present at position 9, the loss of a proton then occurs from N-3.<sup>30</sup> The electron-density values were calculated at various N-atoms of uric acids, indicating that N-7 has lowest value of electron density (Table 2); it is thus expected that the loss of a proton should occur from N-7. However, the H-bonding plays a significant role due to which anion at N-7 does not form; instead, the loss of a proton occurs from N-9.

Controlled potential coulometry of uric acid and various *N*-methylated uric acids at PGE at potentials corresponding to peak  $I_a$  has revealed that all of these compounds oxidized in close to a 1.6±0.2 electron reaction. The electroactive species in all cases has been found to be the conjugate base.

**Spectral Studies.** Spectral changes during electrooxidation were monitored to detect the formation of a UV/vis absorbing intermediate in the reaction. For this purpose, the progress of electrolysis was monitored by recording any

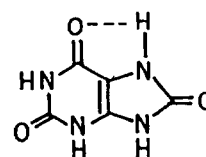


Chart 1.

Table 2. Electron Density Values Calculated for Nitrogen Atoms of *N*-Methyluric acids by MNDO Method

| Compound | N <sub>1</sub> | N <sub>3</sub> | N <sub>7</sub> | N <sub>9</sub> |
|----------|----------------|----------------|----------------|----------------|
| I        | 5.41004        | 5.32138        | 5.21877        | 5.30857        |
| II       | 5.43148        | 5.32686        | 5.21814        | 5.30997        |
| III      | 5.40866        | 5.35822        | 5.22294        | 5.30971        |
| IV       | 5.41186        | 5.32365        | 5.31809        | 5.30385        |
| V        | 5.41064        | 5.32919        | 5.22000        | 5.37227        |
| VI       | 5.43308        | 5.35981        | 5.22199        | 5.30814        |
| VII      | 5.43441        | 5.33051        | 5.31065        | 5.30179        |
| VIII     | 5.41124        | 5.35857        | 5.31833        | 5.31208        |
| IX       | 5.41247        | 5.37075        | 5.23697        | 5.37198        |
| X        | 5.41231        | 5.32936        | 5.30901        | 5.36659        |
| XI       | 5.43544        | 5.36071        | 5.31404        | 5.30940        |
| XII      | 5.44234        | 5.37252        | 5.22588        | 5.36198        |

spectral changes at different time intervals. At pH 7.2, uric acid and its methylated derivatives exhibited two well-defined  $\lambda_{\max}$  at ca. 285–292 and 205–215 nm, and mostly a shoulder at around 232–240 nm. A typical UV-spectrum of compound V (9-methyluric acid), obtained at pH 7.2, is shown by curve 1 in Fig. 2A. Upon applying a potential of 100 mV more positive than the  $E_p$  of peak  $I_a$  at PGE, the absorbance at  $\lambda_{\max}$  292 nm first increased and then decreased systematically (curves 2 to 9). The absorbance in the region 210–270 nm increased systematically and the exhaustively electrolysed solution exhibited  $\lambda_{\max}$  at 218 nm. The change in the adsorbance in the UV spectra is marked by the arrow in Fig. 2. If the potentiostat is open circuited, when the absorbance at  $\lambda_{\max}$  reached to ca. 50% (Curve 4 in Fig. 2A), a systematic decrease in the absorbance was noticed

(Curves 5 to 9 in Fig. 2B). It is thus apparent from the spectral changes that a UV-absorbing intermediate is generated during electrooxidation, which decays in subsequent chemical follow-up reactions. Also, in the case of all *N*-methylated uric acids, a UV-absorbing intermediate has been clearly observed. This generated UV-absorbing intermediate absorbed at longer wavelengths during the electrooxidation of compounds II, IV, and VII. This behavior is similar to that of unsubstituted uric acid,<sup>29</sup> and is due to conjugation present in the imine alcohol intermediate generated in these compounds. In other cases, an imine alcohol intermediate did not absorb at a longer wavelength region.

The kinetics of the decay of the UV-absorbing intermediate generated upon the electrochemical oxidation of uric acid and its *N*-methylated derivatives was monitored by open-circuit relaxation when the absorbance at  $\lambda_{\max}$  decreased to 50%. Studies revealed that in all instances the decomposition of the intermediate species followed first-order kinetics. The pseudo first-order rate constant ( $k$ ) values for the decay of the UV-absorbing intermediate have been calculated from linear plots of  $\log(A - A_{\infty})$  vs. time, and are summarized in Table 3. The value of  $k$  was found to be highest (ca.  $4.2 \times 10^{-3} \text{ s}^{-1}$ ) for 7-methyluric acid (IV), indicating that the imine alcohol intermediate formed in this case is most unstable and undergoes fast hydration. A comparison of the  $k$  values, however, shows no obvious or systematic relationship between the position of methylation and the observed  $k$  values.

The nature of the species generated in peaks  $II_c$  and  $III_c$  reaction at PGE was also studied spectrophotometrically. For this purpose, the spectral changes were monitored for the

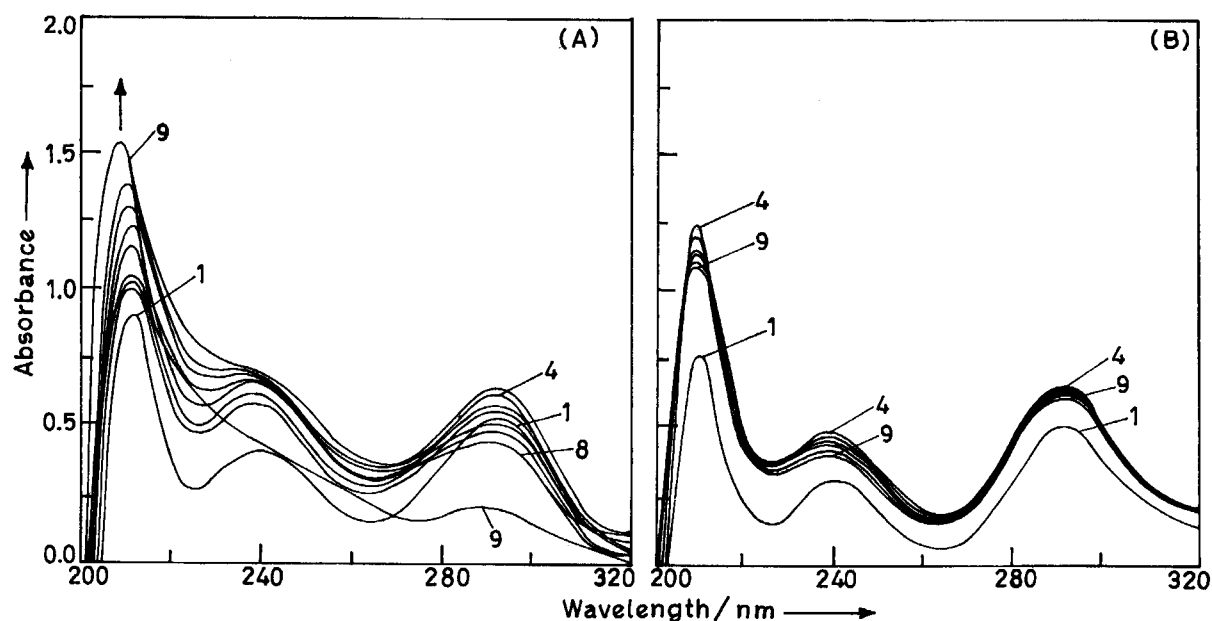


Fig. 2. Spectra observed (A) during and (B) after electrooxidation of 0.1 mM 9-methyluric acid at PGE in phosphate buffer of pH = 7.2. Potential 0.5 V vs. SCE.

(A) Spectra recorded at (1) 0; (2) 5; (3) 10; (4) 15; (5) 25; (6) 35; (7) 50; (8) 70; (9) 160 min of electrolysis.

(B) Spectra recorded after turning off the potential corresponding to curve 4 in (A). Curves were recorded at (5) 5; (6) 10; (7) 20; (8) 35; (9) 50; (10) 80 min of turning off the potential.

Table 3. First-Order Rate Constants Observed for the Decay of the UV-Absorbing Imine Alcohol Intermediate Generated during Electrochemical and Enzymic Oxidation of Various *N*-Methylated Uric Acids at pH 7.2

| Compound | <i>l</i><br>nm | $k^a/10^{-3} \text{ s}^{-1}$ |         |
|----------|----------------|------------------------------|---------|
|          |                | Electrochemical              | Enzymic |
| I        | 236            | 1.0                          | 1.0     |
| II       | 225            | 2.2                          | 2.1     |
|          | 325            | 2.3                          | 2.0     |
| III      | 260            | 3.2                          | 3.3     |
| IV       | 294            | 4.2                          | 3.8     |
| V        | 238            | 1.0                          | 1.2     |
| VI       | 262            | 1.2                          | 1.4     |
|          | 235            | 2.2                          | 1.9     |
|          | 270            | 2.1                          | 1.9     |
| VII      | 295            | 1.9                          | 2.1     |
|          | 239            | 1.5                          | 2.2     |
|          | 293            | 1.5                          | 2.3     |
| VIII     | 260            | 3.0                          | 3.2     |
|          | 290            | 3.3                          | 2.6     |
| IX       | 224            | 2.9                          | 2.8     |
| X        | 220            | 2.9                          | 2.8     |
| XI       | 265            | 2.8                          | 2.3     |
|          | 236            | 2.8                          | 2.9     |
| XII      | 236            | 2.7                          | 2.9     |

a) Average of at least three replicate determinations.

electrooxidation of uric acids (I–XII) at the peak  $I_a$  potentials. When absorbance at the  $\lambda_{\text{max}}$  reduced by ca. 20%, the potential was switched to 100 mV more negative than peak  $II_c/III_c$  potentials and spectral changes were recorded. The results observed for 1,7-dimethyluric acid (VII) are presented in Fig. 3. In all cases, the absorbance at  $\lambda_{\text{max}}$  increased systematically, and a spectrum similar to that of starting compound was obtained. It is thus concluded that the reduction of the UV-absorbing intermediate species generated in the peak- $I_a$  reaction produces the respective starting material.

**Correlation of the Peak Potentials with Energy of the Highest Occupied Molecular Orbital.** The polarographic reduction potential of several aromatic and heterocyclic systems has been found to be related to the electron affinity ( $A$ ), of the molecule by

$$E_{1/2} = A - \Delta E_s, \quad (\text{i})$$

where  $\Delta E_s$  is the difference in the solvation energies of the initial and final product of reduction. The values of the solvation energies remain practically constant for a particular series of compounds if there is no significant change in the size of the substituted and unsubstituted compounds. Several attempts have been made to correlate the reduction potentials with the energy of the lowest free  $\pi$ -molecular orbital.<sup>31</sup> Similarly, it is expected that as electrons are lost from the highest occupied molecular orbital in an oxidation process, a linear correlation should exist between the oxidation potentials and the energy of the highest occupied molecular orbital. In simple molecular theory within Koopman's approximation, the ionization potential is numerically equal to the energy of the

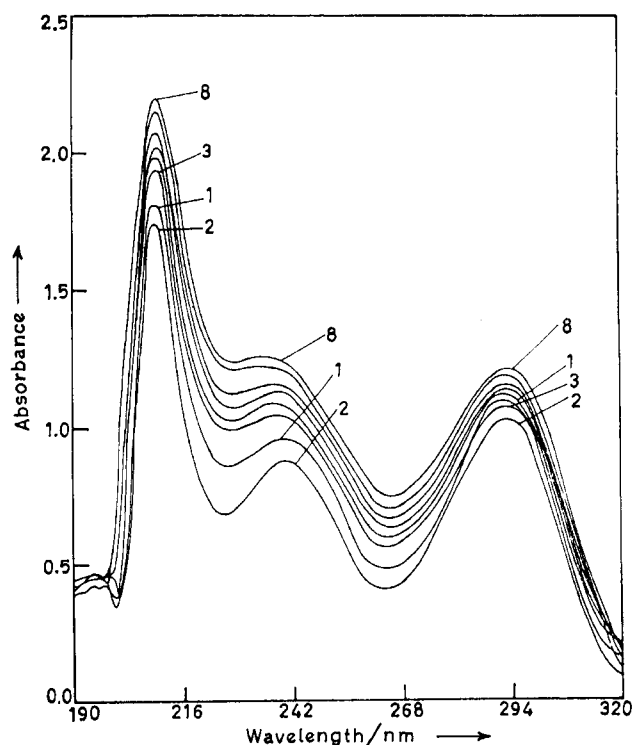


Fig. 3. Spectra observed for the reduction of the UV-absorbing intermediate generated upon electrooxidation of 0.1 mM 1,7-dimethyluric acid at PGE; pH = 7.2. Curve (1) is the spectrum of 1,7-dimethyluric acid before electrolysis. Curve (2) is the spectrum after 30 min of electrolysis at 0.49 V. Curve (3) is the spectrum after 10; (4) 20; (5) 35; (6) 50; (7) 70; (8) 180 min of switching off the potential to  $-1.0 \text{ V}$  vs. SCE.

highest occupied molecular orbital.<sup>32</sup> Thus, for polarographic oxidations the relation

$$E_{1/2}(\text{ox}) = x_n \beta + \Delta E(\text{sol}) + \text{constant} \quad (\text{ii})$$

was found to hold good using the Hückel MO scheme, where  $x_n$  is a number calculated theoretically,  $\beta$  is the resonance integral and  $\Delta E(\text{sol})$  is the difference in the solvation energy between the compound and its positive ion. The small entropy and logarithmic terms are not considered in this relation. A linear correlation was found by Hoytnik<sup>33</sup> between the oxidation potentials obtained by Lund for aromatic hydrocarbons<sup>34</sup> and  $x_n$ , corresponding to the highest occupied molecular orbital.

To correlate the HOMO energies with the electrochemical parameters, the oxidation or reduction potentials should be reversible; however, such correlations have also been attempted in a quasi-reversible system.<sup>35–37</sup> As in the present studies, the oxidation of uric acids has been found to be quasi-reversible at  $100 \text{ mV s}^{-1}$ , and tends to become reversible at higher sweep rates ( $> 1 \text{ V s}^{-1}$ ), the peak potentials of methyl substituted uric acids are correlated to the energy of the highest occupied molecular orbital calculated using the MNDO method.

Because the MNDO scheme provides orbital energies directly in place of the parameter  $x_n$  in the HOMO scheme, Eq.

I may be rewritten in the form

$$(E_{1/2})_{\text{ox}} = a\epsilon_{\text{HOMO}} + b, \quad (\text{iii})$$

where  $a$  and  $b$  are constants.

Figure 4 presents a linear correlation between the oxidation potentials and the energy of the highest occupied molecular orbital for various  $N$ -methyluric acids. The least-squares correlation line can be expressed as

$$E_p = 417.996\epsilon_{\text{HOMO}} + 4215.33. \quad (\text{iv})$$

This correlation clearly explains that the ease of oxidation of  $N$ -methyluric acid is dependent on the energy of HOMO. Thus, with a decrease in the energy of HOMO, oxidation becomes difficult.

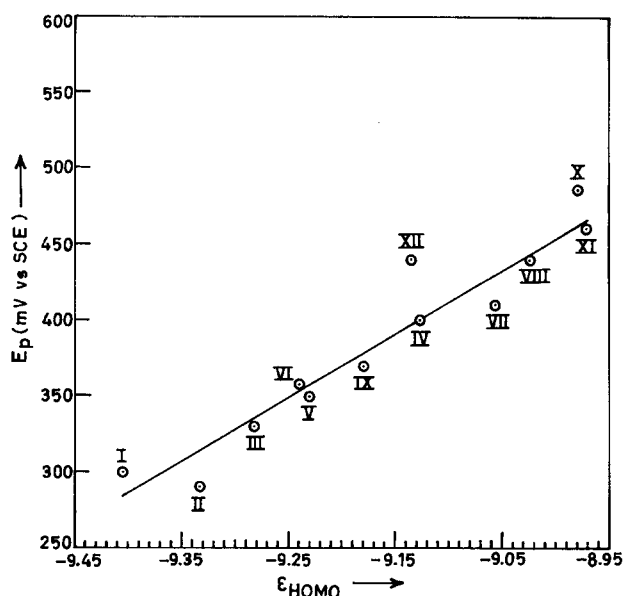


Fig. 4. Plot of oxidation potential ( $E_p$ ) vs. energies of highest occupied MO's for uric acid and its various methylated derivatives.

**Analysis of the Oxidation Products.** The products formed upon the electrooxidation of uric acid and its  $N$ -methylated derivatives corresponding to peak  $I_a$  were separated and characterized at pH 7.2 by  $^1\text{H}$ NMR, GC-MS, HPLC, and related techniques. For providing better insights into the product-characterization process, a typical example of 1,3,9-trimethyluric acid is considered. An exhaustively electrolyzed solution of 1,3,9-trimethyluric acid in gel permeation chromatography gave two peaks. The first peak ( $P_1$ ) was found to be due to phosphate, and was thus discarded. The freeze-dried material obtained under peak  $P_2$  exhibited a single spot in TLC ( $R_f \approx 0.31$ ), and was converted to its trimethylsilyl derivative (see Experimental). The derivatized sample gave only one major peak in GC-Mass at around 25 min, having molar mass of 331 (62%). The molar mass of 331 suggested the product to be 3-methyl-5-hydroxyhydantoin-5-( $N$ -methylcarboxamide) silylated at two positions. The reason for the silylation at only two sites, instead of the three available sites, appears to be the bulky nature of the silyl group, which caused a steric hindrance, thereby preventing silylation of the  $-\text{OH}$  group at position 5. The GC-MS data for the products characterized for other uric acids are summarized in Table 4. A comparison of the obtained products indicated that the presence of methyl groups at the nitrogen of the pyrimidine or imidazole ring of uric acid affects the mechanism of the reaction at the electrode. It is well known<sup>38</sup> that the electrooxidation of uric acid gives 5-hydroxyhydantoin-5-carboxamide and allantoin at physiological pH. Methylation of the pyrimidine  $N$ -atoms significantly affects the ultimate products at pH 7.2. Thus, allantoin was obtained as one of the products only when methyl groups were present only in the imidazole ring. Whenever a methyl group was present in the pyrimidine ring, the only major product formed was the 5-hydroxyhydantoin derivative. This difference in the behavior seems to be due to the influence of the methyl group, which does not permit ring contraction to yield 1-carboxy-3,7-dioxo-2,4,6,8-tetraazabi-

Table 4. Characterization of Silylated Products Formed on the Electrooxidation of Uric Acids at Peak  $I_a$  Potentials by GC-Mass

| Compound | Major products  | $m/z^a$     |
|----------|---|-------------|
| I        | Allantoin,  | 520 (49.0%) |
|          | 5-Hydroxyhydantoin-5-carboxamide                        | 447 (32.3%) |
| II       | 5-Hydroxyhydantoin-5-( $N$ -methylcarboxamide)          | 389 (74.0%) |
| III      | 5-Hydroxyhydantoin-5-carboxamide                        | 447 (9.0%)  |
| IV       | 1-Methylallantoin                                       | 460 (42.2%) |
|          | 5-Hydroxyhydantoin-1-methyl-5-carboxamide               | 389 (33.2%) |
| V        | 1-Methylallantoin                                       | 460 (62.8%) |
|          | 5-Hydroxyhydantoin-3-methyl-5-carboxamide               | 389 (21.5%) |
| VI       | 5-Hydroxyhydantoin-5-( $N$ -methylcarboxamide)          | 389 (76.4%) |
| VII      | 5-Hydroxyhydantoin-1-methyl-5-( $N$ -methylcarboxamide) | 331 (53.0%) |
| VIII     | 5-Hydroxyhydantoin-1-methyl-5-carboxamide               | 389 (7.2%)  |
| IX       | 5-Hydroxyhydantoin-3-methyl-5-carboxamide               | 389 (6.4%)  |
| X        | 1,3-Dimethylallantoin                                   | 402 (22.0)  |
|          | 1,3-Dimethyl-5-hydroxyhydantoin-5-carboxamide           | 331 (17.4%) |
| XI       | 5-Hydroxyhydantoin-1-methyl-5-( $N$ -methylcarboxamide) | 331 (64.0%) |
| XII      | 5-Hydroxyhydantoin-3-methyl-5-( $N$ -methylcarboxamide) | 331 (62.9%) |

a) Relative abundance is shown in parenthesis.

cyclo[3.3.0]oct-4-ene, which is a primary requirement for the formation of allantoin.<sup>38</sup> For all other compounds, properly methylated allantoin and hydroxyhydantoin derivatives were obtained.

**Electrochemical and Enzymic Oxidation: A Comparison.** The spectral changes and decay of the UV-absorbing intermediate generated during enzymic oxidation of these compounds were compared with changes observed during electrooxidation at pH 7.2. A typical comparison of the electrochemical and enzymic oxidation of 1,7-dimethyluric acid is presented in Fig. 5. These spectral changes obtained during enzymic oxidation were similar to those observed during electrochemical oxidation. The above-mentioned results reveal that both processes yield intermediate species which are spectrally identical.

The kinetics of the decay of the UV-absorbing intermediate generated during enzymic oxidation was also studied at selected wavelengths and compared with that generated electrochemically. The change in absorbance with time was monitored at selected wavelengths. Plots of the absorbance vs. time were exponential, thereby indicating that the decomposition of the UV-absorbing intermediate generated enzymically follows first-order kinetics. The values of the rate constant ( $k$ ) for various methylated uric acids during enzymic oxidation are summarized in Table 3. The values of  $k$  for electrochemical and enzymic oxidations are similar.

Thus, the spectral and kinetic studies suggested that a virtually identical intermediate is generated in both oxidations, which decayed at more or less the same rate in a competitive chemical follow-up reaction.

As peak  $I_c$  observed in the cyclic voltammograms of uric acids (Fig. 6) was found to be due to the reduction of species

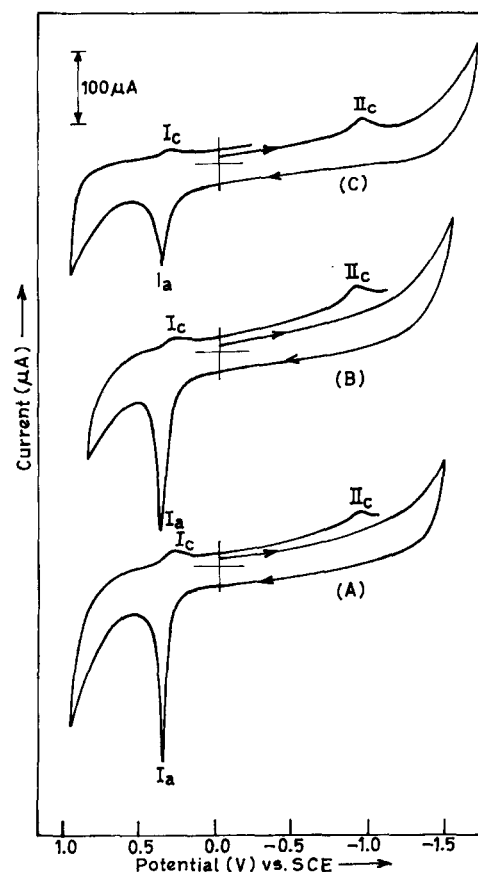


Fig. 6. Cyclic voltammograms observed during enzymic oxidation of 1,3-dimethyluric acid at pH 7.2. (A) 0.1 mM 1,3-dimethyluric acid. (B) After adding 0.002 mM horseradish peroxidase. (C) 5 min after adding 0.6 mM  $H_2O_2$  in (B).

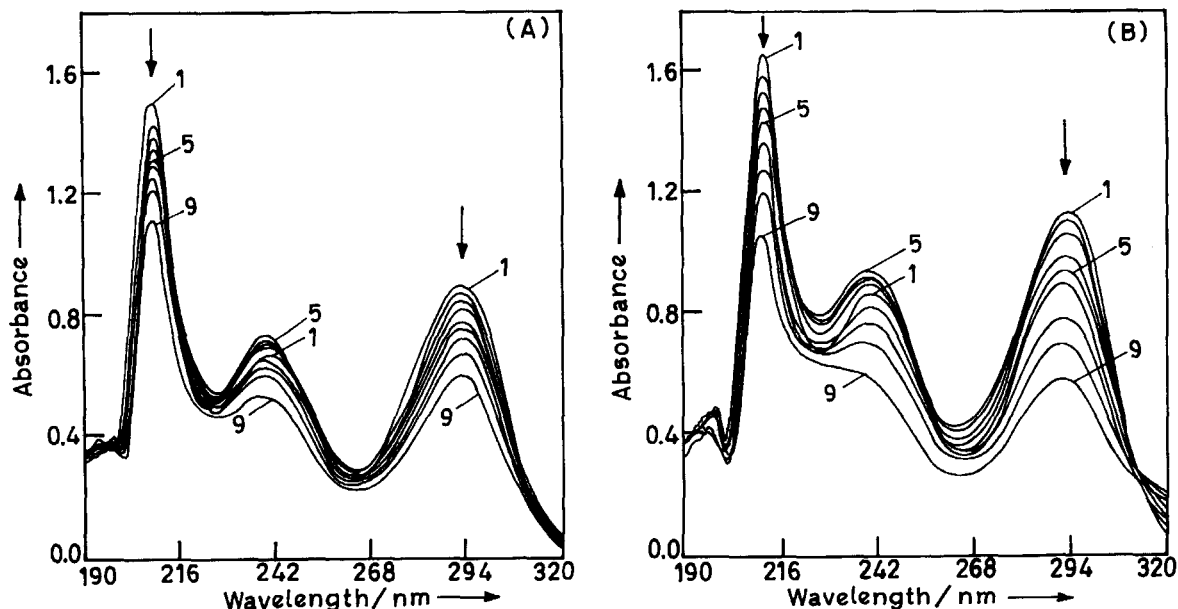


Fig. 5. A comparison of spectral changes observed during electrochemical and enzymic oxidation of 0.1 mM 1,7-dimethyluric acid at pH 7.2. Spectra were recorded at:

(A) (1) 0; (2) 5; (3) 10; (4) 15; (5) 25; (6) 30; (7) 40; (8) 50; (9) 80 min of initiating enzymic oxidation.

(B) (1) 0; (2) 5; (3) 10; (4) 25; (5) 35; (6) 55; (7) 75; (8) 90; (9) 120 min of electrolysis.

generated in the peak- $I_a$  reaction, the cyclic voltammetric changes were monitored during enzymic oxidation in order to detect peak  $II_c$ . In cyclic voltammetry, when the sweep was initiated towards a negative potential, peak  $II_c$  was never obtained in the first negative sweep. However, after the addition of  $H_2O_2$ , peak  $II_c$  started to appear in the first negative sweep at the same potential as that observed during the electrochemical oxidation of the compound. The cyclic voltammograms recorded during enzymic oxidation of 1,3-dimethyluric acid at pH 7.2 are shown in Fig. 6. It was thus inferred that a species, reducible at peak  $II_c$  potentials, is generated during enzymic oxidation, which is similar to that generated electrochemically. As both of the species are same, their reductions are observed in peak  $II_c$  at exactly similar potentials.

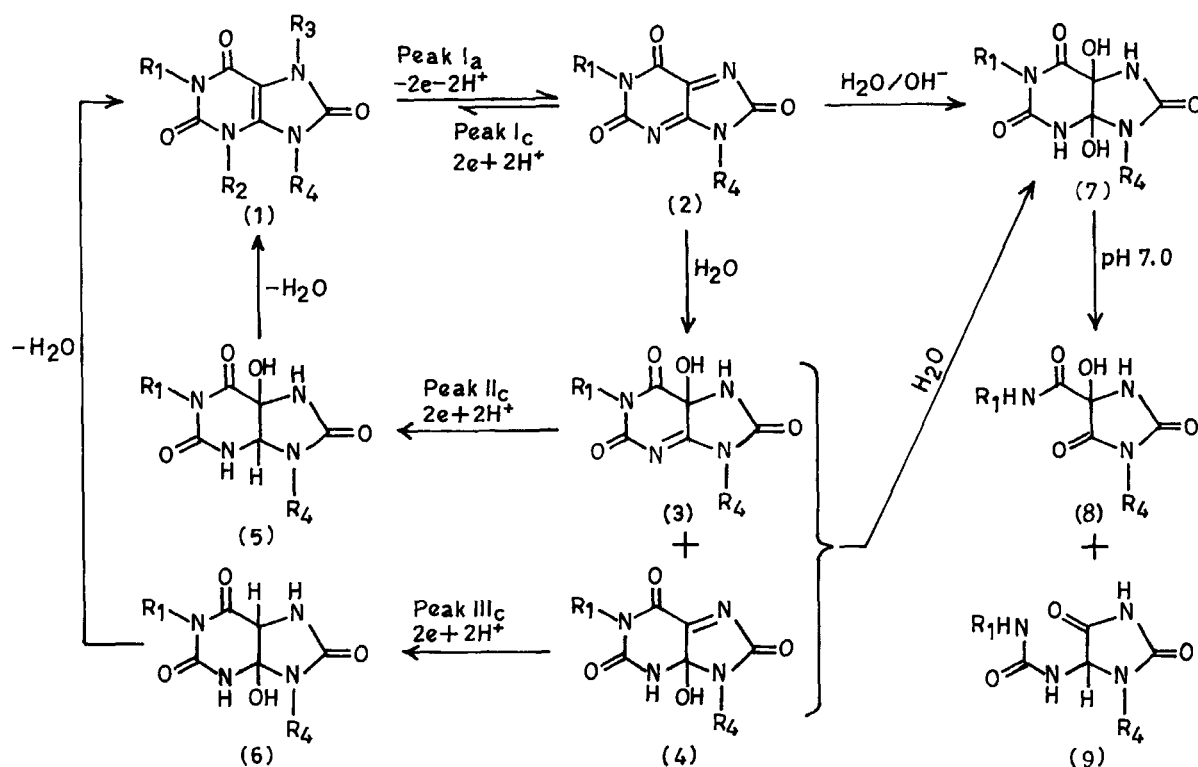
Electrochemical oxidation has revealed that cyclic voltammetric peak  $II_c$  is due to the reduction of imine alcohol. It thus seems reasonable to conclude on the basis of the identical UV-spectral changes,  $k$  values and the appearance of peak  $II_c$  during enzymic and electrochemical oxidation that the peroxidase catalysed oxidation of *N*-methylated uric acids also generates an imine alcohol intermediate, and follows a pathway similar to that of electrochemical oxidation.

### Conclusion

An analysis of different results obtained voltammetrically, spectrally, and product characterization indicates that the oxidation of all *N*-methylated uric acids occur in a 2e quasi-reversible step to give a diimine species. The 2e oxidation

of uric acid has been reported to proceed in two 1e transfer reactions, leading to the formation of diimine via a cationic free radical.<sup>39</sup> The loss of two protons during oxidation occurs from the N-7 and N-9 positions when  $R_3$  and  $R_4 = H$ . If methyl groups are present at these positions, the loss of a proton occurs from N-3 and 2e,  $H^+$  oxidation gives diimine (2). The formed diimine is unstable as the half life of diimines generated during 2e,  $2H^+$  oxidation of uric acid and 3,7-dimethyluric acid have been found to be 20–30 ms.<sup>40</sup> The diimines are then attacked by water to first give imine alcohol and then the diol.

A general mechanism for the oxidation of *N*-methyluric acid is presented in Scheme 1, considering  $R_1 = R_4 = CH_3$  and  $R_2 = R_3 = H$ . As the nature of the electrode reaction was established as EC, the subsequent formation of imine alcohol (3 and 4) from diimine (2) is the chemical follow-up step. The reduction of species 3 and 4 is possible because both possess an unsaturated  $-C=N$  linkage. However, in uric acids this reduction is observed at higher negative potentials as compared to the usual  $-C=N-$  reduction potentials observed in other compounds by Zuman et al.<sup>28</sup> One of the reasons for such a behavior is the possibility of methylated imines to be protonated, due to the presence of the  $-CH_3$  group at N-atoms. The  $pK_a$  of such protonated imines has been found to be  $> 11.0$ .<sup>41</sup> The values of the electron density calculated (Table 2) at the nitrogen atoms also indicate that methyl substitution at N-9 significantly increase the electron density at this position. In uric acid ( $R_1, R_2, R_3, R_4 = H$ ), only one reduction peak was noticed in CV, whereas 1,3,7- and 1,3,



Scheme 1. Tentative general reaction mechanism proposed for the electrochemical oxidation of *N*-methyluric acids when  $R_1 = R_4 = CH_3$  and  $R_2 = R_3 = H$ .



9-trimethylated uric acids always exhibited two reduction peaks,  $II_c$  and  $III_c$ . The appearance of two reduction peaks in such cases can be attributed to the steric hindrance caused by the methyl groups which separates the reduction potential of two C=N double bonds between positions 3,4 and 5,7 atoms. The reduction of C=N in species **4** in a  $2e^-$ ,  $H^+$  reaction will give dihydro species **5** and **6**, respectively, which upon losing a water molecule, form the starting compound **1**. The diol (**7**) upon decomposition in a series of reactions gives different final products (**8** and/or **9**), depending upon the position of the methyl groups, as presented in Table 4.

Thus, on the basis of the results reported concerning the electrooxidation of various *N*-methylated derivatives, it can be concluded that the methyl group in uric acids besides producing an electron releasing effect and making oxidation difficult, also restricts the number of resonating structures. In addition, *N*-methylation affects the rate of decomposition of the UV-absorbing intermediate and alters the course of the mechanism leading to the formation of different products. However, the natures of the primary electrode reaction and the follow-up chemical reaction remain the same.

Comparative studies on electrochemical and enzymic oxidation reveals that the peroxidase catalyzed oxidation of *N*-methyluric acids proceeds by a mechanism similar to that of electrochemical oxidation. Thus, the present studies support the view that the electrochemical and enzymic processes proceed in a chemical sense by an identical mechanism, and that electrochemical studies can be used to understand the chemical aspects of the peroxidase catalyzed oxidation.

The following significant information has been deduced from the present studies:

(a) The electron-density calculations at various atoms of *N*-methyluric acids strongly indicate that the presence of methyl groups in the imidazole ring increases the electron density at the N-7 and N-9 positions. On the other hand, the presence of methyl groups in the pyrimidine ring does not increase the electron density at the N-1 or N-3 positions, because N-1 is flanked between two  $>C=O$  groups and N-3 has an adjacent  $>C=O$  group and  $\pi$ -conjugation transfers the electron density to oxygen attached to position 6.

(b) The methyl group at position 1 and/or 3 does not permit ring contraction of the pyrimidine ring, and hence the major product in such cases is only 5-hydroxyhydantoin derivative.

(c) A linear correlation is observed between the peak potentials of *N*-methyluric acids with the energy of the highest occupied molecular orbital using MNDO calculations.

(d) The values of  $\Delta E_p$  followed the additivity only when two methyl groups were present in different rings of uric acids.

Thus, from the present investigation it can be concluded that MO calculations together with electrochemical and other spectroscopic characteristics could provide deep insight into the redox chemistry of the present series of methylated uric acid. It is also reasonable to deduce that the solid electrode used can mimic the active site of an enzyme in oxidizing simple biomolecules. It may also be mentioned that more than

one pathway is always possible for the formation of products. However, the proposed mechanism explains all of the observed voltammetric, coulometric, and spectral behavior.

N. J. is thankful to the Council of Scientific and Industrial Research, New Delhi for the award of a Research Associateship. Thanks are due to the Director, I. I. P., Dehradun for permitting GC-Mass studies. Financial assistance for this work was provided by A.I.C.T.E., New Delhi through grant No. 8017/RDII/R&D/TAP(937)/98-99.

## References

- 1 E. S. West and W. R. Todd, "Textbook of Biochemistry," Macmillan Company, N.Y. (1963).
- 2 E. Bonora, G. Targhar, M. B. Zener, F. Saggiani, V. Cacciatori, F. Tosi, D. Travia, M. G. Zenti, P. Branzi, and L. Santi, *Int. J. Obesity*, **20**, 975 (1996).
- 3 K. Nishioka, *Rinsho Kensa*, **37**, 253 (1993).
- 4 K. Fabian, D. Schlegel, B. Hauptmann, and H. Zerber, *Dtsch. Z. Sportmed.*, **44**, 5 (1993).
- 5 B. N. Ames, R. Cathcart, E. Schwiers, and P. Hochstein, *Proc. Natl. Acad. Sci. U.S.A.*, **78**, 6858 (1981).
- 6 M. Griffiths, *J. Biol. Chem.*, **172**, 853 (1948).
- 7 R. N. Goyal and A. Kumar, *Indian J. Chem.*, **28**, 948 (1989).
- 8 F. Ardi, *Biophys. Chem.*, **44**, 143 (1992).
- 9 C. Londons and J. Wolff, *Proc. Natl. Acad. Sci. U.S.A.*, **74**, 5482 (1977).
- 10 M. Williams, *Neurochem. Int.*, **14**, 249 (1989).
- 11 N. Svedmyr, K. E. Andersson, and G. A. Persson, "Excerpta Medica," Amsterdam (1985), p. 135.
- 12 S. R. R. Musk and G. G. Steel, *Int. J. Rad. Bio.*, **57**, 1105 (1990).
- 13 J. V. Arnanada and T. Thurman, *Clin. Perinat.*, **6**, 87 (1969).
- 14 Y. Nishida, *J. Pharm. Pharmacol.*, **43**, 885 (1991).
- 15 J. M. Zen and C. T. Hsu, *Talanta*, **46**, 1363 (1998).
- 16 J. Odo and H. Hashimoto, *Anal. Sci.*, **14**, 935 (1998).
- 17 Y. Q. Zhang, R. A. Gu, W. D. Shen, and X. J. Zheng, *Anal. Lett.*, **32**, 251 (1999).
- 18 A. N. Araujo, J. A. M. Catita, and J. L. F. C. Lima, *Anal. Sci.*, **14**, 809 (1998).
- 19 Y. X. Song, H. X. Zhang, and M. C. Liu, *Fenxi Huaxue*, **27**, 243 (1999).
- 20 Z. Yan, J. R. Zhang, and H. Q. Fang, *Anal. Lett.*, **32**, 223 (1999).
- 21 R. N. Goyal, A. K. Jain, and N. Jain, *J. Chem. Soc., Perkin Trans. 2*, **1995**, 1055.
- 22 J. Abe, Y. Nagasawa, and H. Takahashi, *J. Chem. Phys.*, **91**, 3431 (1989).
- 23 G. D. Christian and W. C. Purdy, *J. Electroanal. Chem.*, **3**, 363 (1982).
- 24 J. J. Lingane, "Electroanal. Chemistry," Wiley Interscience, N.Y. (1966).
- 25 M. J. S. Dewar and W. Thiel, *J. Am. Chem. Soc.*, **99**, 4899 (1977).
- 26 D. J. Sutor, *Acta Crystallogr.*, **11**, 83 (1958).
- 27 P. H. Rieger, "Electrochemistry," Prentice Hall, N. J. (1987), p. 343.
- 28 P. Zuman, "Substituents Effects in Organic Polarography," Plenum Press, N.Y. (1967).
- 29 M. Z. Wrona, J. L. Owens, and G. Dryhurst, *J. Electroanal.*

*Chem.*, **105**, 295 (1979).

30 F. Bergmann and S. Dikstein, *J. Am. Chem. Soc.*, **77**, 691 (1955).

31 O. Chalvet and I. Jano, *Compt. Rend.*, **259**, 1867 (1964).

32 A. Streitwieser, "Molecular Orbital Theory for Organic Chemists," John Wiley and Sons, N.Y. (1962).

33 G. J. Hoytnik, *Adv. Electrochem. Electrochem. Eng.*, **7**, 221 (1970).

34 H. Lund, *Acta Chem. Scand.*, **11**, 1323 (1957).

35 E. S. Pysh and N. C. Yang, *J. Am. Chem. Soc.*, **85**, 2124 (1963).

36 B. Pullman and A. Pullman, "Quantum Biochemistry,"

Wiley Interscience, N.Y. (1963).

37 M. Lalithambika and S. K. Sinha, *Z. Phys. Chem.*, **94**, 127 (1975).

38 R. N. Goyal, A. B. Toth, G. Dryhurst, and N. T. Nguyen, *Bioelectrochem. Bioenerg.*, **9**, 39 (1982).

39 R. N. Goyal, S. Ahmad, and A. Rastogi, *Indian J. Chem., Sect. A*, **36A**, 283 (1997).

40 J. L. Owens, H. H. Thomas, and G. Dryhurst, *Anal. Chim. Acta*, **96**, 89 (1978).

41 D. D. Perrin, B. Dempsey, and E. P. Serjeant, "pK<sub>a</sub> Prediction for Organic Acids and Bases," Chapman and Hall, London (1981), p. 19.

---